The theoretical study on interaction of hydrogen with single-walled boron nitride nanotubes. I. The reactive force field $ReaxFF_{HBN}$ development

Sang Soo Han, Jeung Ku Kang, and Hyuck Mo Lee[a)]
Department of Materials Science and Engineering, Korea Advanced Institute of Science and Technology (KAIST), Daejeon 305-701, Republic of Korea

Adri C. T. van Duin and William A. Goddard III
Materials and Process Simulation Center, California Institute of Technology, California 91125

(Received 2 November 2004; accepted 21 June 2005; published online 19 September 2005)

We present a new reactive force field $ReaxFF_{HBN}$ derived to accurately model large molecular and condensed phase systems of H, B, and N atoms. $ReaxFF_{HBN}$ has been tested against quantum calculation data for B–H, B–B, and B–N bond dissociations and for H–B–H, B–N–B, and N–B–N bond angle strain energies of various molecular clusters. The accuracy of the developed $ReaxFF_{HBN}$ for B–N–H systems is also tested for (i) H–B and H–B bond energies as a function of out of plane in $H-B(NH_2)_3$ and $H-N(BH_2)_3$, respectively, (ii) the reaction energy for the $B_3N_3H_6+H_2 \rightarrow B_3N_3H_8$, and (iii) crystal properties such as lattice parameters and equations of states for the hexagonal type (*h*-BN) with a graphite structure and for the cubic type (*c*-BN) with a zinc-blende structure. For all these systems, $ReaxFF_{HBN}$ gives reliable results consistent with those from quantum calculations as it describes well bond breaking and formation in chemical processes and physical properties. Consequently, the molecular-dynamics simulation based on $ReaxFF_{HBN}$ is expected to give a good description of large systems (>2000 atoms even on the one-CPU machine) with hydrogen, boron, and nitrogen atoms. © *2005 American Institute of Physics*.
[DOI: 10.1063/1.1999628]

I. INTRODUCTION

The aim of the work described here is to develop the multiscale computational frame usable to describe chemical processes and physical properties for large systems of H, B, and N atoms with the accuracy of the first-principles methods, but with the efficiency of a force field-based molecular-dynamics simulation method. For example, a quadratic configuration-interaction (QCISD(T)) (Ref. 1) method, including both single and double excitations and connected triples, have proven remarkably accurate. On the other hand, the computational time for this *ab initio* method is proportional to O^3V^4 where O and V are the number of occupied and virtual orbitals, respectively. Consequently, QCISD(T) is limited in application to small chemical systems due to its computational complexity and expense. Also, the development of density-functional theory (DFT) techniques, for example, B3LYP,[2] has resulted in methods that are significantly more efficient than *ab initio* methods of comparable accuracy. However, any current DFT method is still not fast enough to describe chemical and physical properties accurately. Consequently, there is currently no computational method that is both chemically accurate and computationally efficient enough to be applied to large, dynamic systems with a few thousand to million atoms of boron, nitrogen, and hydrogen elements.

The boron nitrogen systems have several condensed allotropes such as tubular and conical forms, and other polymorphs of a zinc-blende type (*c*-BN), a wurtzite type (*w*-BN), a graphite type (*h*-BN), and a rhombohedra type (*r*-BN). The *h*-BN crystal has a stacking sequence of *AaAa*,…, while the *r*-BN crystal has a three-layer sequence of *ABCABC*,… .[3–7] Since the discovery of the boron nitride nanotube (BNNT) in 1995,[3] there has been great interest in the BNNT because it has about 5.5-eV band gap irrespective of its helicity. This is a very promising property in that the BNNT can be more cheaply developed for nanometer scale size transistors than carbon nanotubes (CNTs). This is because the band gap of CNTs varies significantly depending on its chirality.[8] In addition, modification of the x, y, and z stoichiometries of $B_xC_yN_z$ nanotubes also presents a means to tailor their electronic properties.[9] Also it was recently reported from theoretical studies that BN fullerene materials have hydrogen storage capacities larger than carbon fullerene materials.[10,11] Ma *et al.*[12] showed that their multiwalled bamboolike BNNTs had the hydrogen storage capacity of about 2.6 wt % at room temperature. On the other hand, Tang *et al.*[13] found that their BNNTs with collapsed structures absorbed 4.2-wt % hydrogen at room temperature. These results show that BNNTs have great potentials to be used as hydrogen storage media. Moreover, the synthesis of a *c*-BN crystal has recently gained an increased interest in a wide range of areas stemming from its extreme hardness, wide band gap, high thermal conductivity, and chemical inertness.[14] There have been some reports on the synthesis of boron nitride films by employing physical and chemical-

[a)]Electronic mail: hmlee@kaist.ac.kr

TABLE I. Atom parameters (energies are in units of kcal/mol).

Atom	$p_{ov/un}$	p_{under}	$p_{v,3}$[a]	$p_{v,5}$[a]	$p_{v,6}$[a]
B	−2.50	31.91	3.96	3.00	2.84

[a]Used for all the valence angles when the B atom is in a central position.

vapor deposition techniques.[15–17] However, the boron nitride thin films synthesized so far exhibit multilayered structures with different phases.[18,19] The interfacial region next to the substrate was usually an amorphous layer of a few nanometers, on the top of which was a textured *h*-BN layer, and a *c*-BN layer was observed upon the *h*-BN layer. Harris *et al.*[20] used hydrogen for etching and found that hydrogen could remove other phases except the *c*-BN phase. Consequently, the selectivity of hydrogen in etching BN phases is considered to be the key factor for success in synthesizing of high-quality *c*-BN films.

The molecular-dynamics simulation studies using DREIDING (Ref. 21) and universal force field[22] (UFF) have been reported on large systems of boron, nitrogen, and hydrogen elements, but the results based on conventional force fields[21,22] are not considered to give a reliable and accurate description of chemical reactivity. In this respect, the ReaxFF (Refs. 23–26) has been recently proposed to describe well bond breaking and bond formation in chemical processes, from which the conventional force fields are suffering, as well as the crystal and mechanical properties for condensed phases accurately.[23,24,26]

In this study we develop and present the new reactive force field, called "ReaxFF$_{HBN}$," to allow accurate description of chemical processes and physical properties for large systems with hydrogen, boron, and nitrogen atoms. The ReaxFF$_{HBN}$ parameters are derived against the data from quantum simulations of various molecules, clusters, and condensed phases. The accuracy of the new parameter set is also tested in several cases, including (i) H–B and H–N bond energies as a function of out of plane in $H-B(NH_2)_3$ and $H-N(BH_2)_3$, respectively, (ii) the reaction energy for the chemical reaction $B_3N_3H_6+H_2 \rightarrow B_3N_3H_8$, and (iii) crystal properties such as lattice parameters and equations of states for *h*-BN and *c*-BN crystals.

Section II describes the theory and computational details of the present force field. Section III reports and discusses the results of this approach and we conclude with Sec. IV.

II. THE PRESENT FORCE FIELD

The ReaxFF$_{HBN}$ framework was initially developed for hydrocarbons.[23] Since then it has been successfully employed in the study of Si/SiO_2 (Ref. 24) and Al/Al_2O_3 (Ref. 25) interfaces. As described in Refs. 23 and 24, the total energy in the ReaxFF is partitioned into several energy terms as given in Eq. (1),

$$E_{system} = E_{bond} + E_{over} + E_{under} + E_{lp} + E_{val} + E_{pen} + E_{tors} + E_{conj} + E_{vdWaals} + E_{Coulomb}. \quad (1)$$

The detailed description for each term was described in the Refs. 23 and 24. On the other hand, ReaxFF$_{HBN}$ is derived for the systems of hydrogen, boron, and nitrogen atoms using the above framework. Parameters for ReaxFF$_{HBN}$ (see Tables I–VII) are determined through optimization against DFT data. The bond, angle, and torsion parameters for nitrogen and hydrogen atoms are taken from the force field used in the nitramine hexahydro-trinitro-triazine (RDX) study.[25] However, we optimize parameters for B atom, including B–B, B–H, and B–N bonds; H–B–H, B–N–B, N–B–N, H–B–N, and H–N–B angles; and all torsion angles with a central B–B and B–N. For the cluster systems, DFT calculations are performed on the JAGUAR program[27] using the B3LYP (Ref. 2) method with a triple-zeta Pople basis set of 6-311G**.[28] For boron nitride crystals, we fit two phases of the *h*-BN crystal (3) and the *c*-BN crystal (4), where the numbers in parentheses mean the coordination numbers of B or N atom. The ReaxFF was shown to describe well the variation of the coordination numbers of one atom in the crystal.[23–26] For DFT calculations on condensed periodic systems we employ the generalized gradient approximation (GGA) based on the Perdew-Wang functional[29] for the exchange-correlation potential with ultrasoft pseudopotentials[30] to replace the core electrons, which is implemented in the CASTEP program.[31] We use a kinetic-energy cutoff of 480.0 eV and the Monkhorst-Pack scheme[32] to generate the *k*-space grid. It is found that a *k*-point sampling of $4\times4\times4$ is sufficient for energy convergence. In addition a successive one-parameter search technique[33] is used to optimize the force field parameters.

TABLE II. Coulomb and 1–3 bond order correction parameters

	Coulomb parameters			1-3 BO correction		
Atom	η (eV)	χ (eV)	γ (Å)	λ_3	λ_4	λ_5
B	7.18	1.88	0.57	7.25	7.53	0.52

TABLE III. van der Waals and bond radius parameters.

Atom	r^{σ} (Å)	r^{π} (Å)	r_{vdW} (Å)	*ee* (kcal/mol)	*aa*	γ_w (Å)
B	1.30	1.00	1.65	0.08	13.00	2.00

III. RESULTS AND DISCUSSION

A. Bond dissociation

First, DFT calculations are carried out to determine bond dissociation energies for B–B, B–H, and B–N bonds. Next, these results are used to derive the parameters for ReaxFF$_{HBN}$. In performing DFT calculations, we determined ground-state structures through full geometry optimizations.

TABLE IV. Bond energy parameters (D_e^{σ} and D_e^{π} are in units of kcal/mol).

Bond	D_e^{σ}	D_e^{π}	$p_{be,1}$	$p_{be,2}$
B–B	131.78	···	0.96	0.40
B–H	166.76	···	−0.50	5.83
B–N	162.17	91.61	0.64	0.98

TABLE V. Bond order parameters.

Bond	$p_{bo,1}$	$p_{bo,2}$	$p_{bo,3}$	$p_{bo,4}$
B–B	−0.10	4.73	⋯	⋯
B–H	−0.05	5.37	⋯	⋯
B–N	−0.11	7.60	−0.10	17.10

Then, dissociation profiles are constructed through total-energy calculations at the modified geometries only by changing the bond length. The dissociation curves are also determined with the singlet and triplet states on DFT calculations. To optimize the $\text{ReaxFF}_{\text{HBN}}$ parameters, we used the DFT results of the singlet state from the equilibrium distance up to the dissociation limit with the lowest of either the singlet or triplet state energy.

Figure 1 and Table VIII describe the simulation results obtained using the $\text{ReaxFF}_{\text{HBN}}$ parameters for the B–B bond dissociation in the H_2B-BH_2 system. The B–B bond distance of 1.74 Å and the bond energy of 96.2 kcal/mol using DFT are shown to be similar to the $\text{ReaxFF}_{\text{HBN}}$ values of 1.76 Å and 90.6 kcal/mol, respectively. All dissociation curves except the H_2B-BH_2 system, studied in this work, are given in Figs. 1–5 on EPAPS.[34] Table VIII also shows the B–H bond dissociation modeled using BH_3 system. In this case, $\text{ReaxFF}_{\text{HBN}}$ predicts the equilibrium bond distance of 1.17 Å and the bond dissociation energy of 106.5 kcal/mol. The good agreement is also observed with DFT values of 1.19 Å and 111.0 kcal/mol. To model another B–H bond, we adopt a borazine molecule of $B_3N_3H_6$ that is the smallest cluster of the BNNT. As shown in Table VIII, $\text{ReaxFF}_{\text{HBN}}$ reproduces the B–H bond energy and the geometries similar to DFT data. We also considered the B–H bond dissociation for a BH_4 radical. According to the valence bond theory, the BH_4 radical was predicted not to exist. However, electron-spin-resonance (ESR) spectroscopy studies[35–37] show the existence of the BH_4 radical and it is suggested that the lone electron interacts strongly with two equivalent H atoms. In addition full electronic structure calculations[38–40] reveal that the ground state of the BH_4 radical has a C_{2v} symmetry. The predicted BH_4 radical geometry[40] using the MP2/6−311++G(d,p) method is found to agree well with those by the $\text{ReaxFF}_{\text{HBN}}$ and B3LYP/6−311G** calculations. In the case of the B–N bond dissociation modeled using the H_2B-NH_2 cluster, DFT gives its B–N bond length and dissociation energy of 1.39 Å and 149.2 kcal/mol, respectively, whereas $\text{ReaxFF}_{\text{HBN}}$ does give its corresponding values of 1.42 Å and 147.7 kcal/mol, as shown in Table VIII. Using a HB=NH cluster we also investigate the B=N bond dissociation behavior and find that $\text{ReaxFF}_{\text{HBN}}$ is good to describe the B=N bond dissociation, as given in Table VIII.

Along with valence interactions which depend on overlap, there are repulsive interactions at short interatomic distances due to Pauli principle orthogonalization, as well as attraction energies at long distances due to dispersion. This van der Waals interaction at long distances is included for *all* atom pairs to avoid awkward alterations in the energy description during bond dissociation.

TABLE VI. Valence angle parameters.

Angle	$\Theta\Theta_{0,0}$	k_a	k_b	$p_{v,1}$	$p_{v,2}$	$p_{v,4}$	p_{pen}
H–B–H	53.37[a]	15.84	1.19	0.00	2.06	1.69	0.00
B–N–B	50.00	40.00	0.74	0.00	2.25	1.20	0.00
N–B–N	50.17	40.00	1.15	0.00	1.73	1.25	0.00
H–B–N	59.45	40.00	3.53	0.00	1.85	1.04	0.00
H–N–B	83.67	13.03	1.14	0.00	1.57	1.43	0.00

[a]This value leads to the equilibrium angle of 126.63° for the H–B–H valence angle.

TABLE VII. Torsion angle parameters (V_1, V_2, and V_3 are in units of kcal/mol).

Torsion angle	V_1	V_2	V_3	p_t	p_{conj}
X–B–B–X[a]	0.00	50.00	0.00	−4.00	0.00
X–B–N–X[b]	0.00	50.00	0.00	−4.00	0.00

[a]Used for all the torsion angles having a central B–B bond.
[b]Used for all the torsion angles having a central B–N bond.

B. Valence angle terms

Angle bend energies for $\text{ReaxFF}_{\text{HBN}}$ have been determined using various clusters of boron, nitrogen, and hydrogen atoms. There are 12 different valence angle cases (X-Y-Z) (excluding Y=H). Of all these 12 cases, parameters of only five cases, H–B–H, B–N–B, N–B–N, H–B–N, and H–N–B, are optimized in this work. Three cases of N–N–N, H–N–H, and H–N–N were already parametrized in the previous study,[25] while other parameters of B–B–B, B–N–N, N–B–B, and H–B–B remain to be investigated in the future works.

First, the various clusters are fully optimized through DFT calculations. Then, single-point calculations are performed at the modified geometries by changing only the valence angles from optimized geometries. As a representative, we determine parameters of the H–B–H valence angle term using a BH_3 molecule in Fig. 2. For the BH_3 cluster, DFT gives an equilibrium B–H bond length of 1.19 Å and its H–B–H angle of 120.0° (Table VIII). Next, any one of three

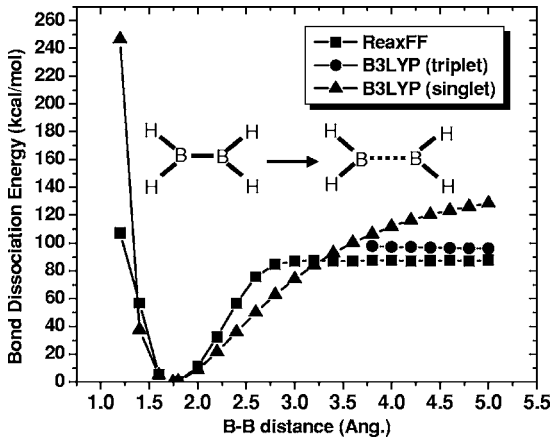

FIG. 1. B3LYP and $\text{ReaxFF}_{\text{HBN}}$ data for dissociation of B–B bond in the H_2B-BH_2 cluster.

TABLE VIII. Bond dissociation energies as well as bond distances and angles used for the optimized parameters for $ReaxFF_{HBN}$ (the geometries are shown in Fig. 1). Energies are in units of kcal/mol.

Formula	Dissociation energy				Bond distance and angle		
H_2B-BH_2	Reactant	Product	B3LYP	ReaxFF	Geometry	B3LYP	ReaxFF
	H_2B-BH_2	H_2B+BH_2	96.19	90.59	B–B (Å)	1.74	1.76
					B–H (Å)	1.19	1.17
					∠H–B–H (°)	116.2	120.4
BH_3	BH_3	BH_2+H	110.97	106.46	B–H (Å)	1.19	1.17
					∠H–B–H (°)	120.0	120.1
$B_3N_3H_6$	$B_3N_3H_6$	$B_3N_3H_5+H$	112.54	103.31	B–N (Å)	1.43	1.38
					B–H (Å)	1.19	1.21
					N–H (Å)	1.01	1.01
					∠B–N–B (°)	122.9	122.5
					∠N–B N (°)	117.1	117.5
BH_4	BH_4	BH_3+H	28.31	30.41	B–H1 (Å)	1.18	1.18
					B–H2 (Å)	1.29	1.83
					∠H1–B–H1 (°)	128.7	120.2
					∠H1–B–H2 (°)	113.1	118.3
					∠H2–B H2 (°)	49.4	38.4
H_2B-NH_2	H_2B-NH_2	H_2B+NH_2	149.21	147.68	B–N (Å)	1.39	1.42
					B–H (Å)	1.19	1.21
					N–H (Å)	1.01	1.04
					∠H–B–H (°)	119.1	121.5
					∠H B–N (°)	121.8	126.2
					∠H N–B (°)	123.2	121.3
HB═NH	HB–NH	HB+NH	227.81	225.19	B–N (Å)	1.23	1.22
					B H (Å)	1.17	1.16
					N–H (Å)	0.99	1.06
					∠H–B–N (°)	180.0	127.8
$H_2B-NH-BH_2$					B–N (Å)	1.42	1.44
					B H (Å)	1.19	1.19
					N–H (Å)	1.02	1.09
					∠B–N–B (°)	126.4	126.5
$H_2N-BH-NH_2$					B–N (Å)	1.42	1.44
					B–H (Å)	1.20	1.23
					N–H (Å)	1.01	1.02
					∠N–B–N (°)	123.2	121.1

H–B–H angles is changed with keeping three B–H bond lengths fixed and we perform single-point energy calculation at this distorted configuration. Figures 6 and 7 on EPAPS (Ref. 34) compare the $ReaxFF_{HBN}$ energies with DFT energies for the B–N–B and N–B–N valence angle terms.

We also use a borazine molecule to determine the valence energy terms (see Fig. 8 on EPAPS).[34] First, the borazine molecule is fully optimized using DFT. Next, the B–N–B angle is changed while we make the B–H, N–H, and B–N bond lengths fixed, where B–N–B, H–B–N, and H–N–B angles move automatically with their corresponding angle changes. In this case, $ReaxFF_{HBN}$ gives reliable results to the DFT distortion energies for the borazine when the B–N–B angles are in the range from 122.9° to 90.0°, but it underestimates the DFT energies when the angles become less than 90.00°.

C. Charge distributions

According to previous works,[41,42] the B–N bonds of the BNNT were found to be ionic rather than covalent. Consequently, we employ $ReaxFF_{HBN}$ for a better description of the charges for the BNNT. In $ReaxFF_{HBN}$, the electronegativity equalization method (EEM) scheme[43] is used to determine the charge distributions. EEM parameters (electronegativity χ, chemical hardness η, and shielding radius γ) are optimized against CHELPG (Ref. 44) charges obtained

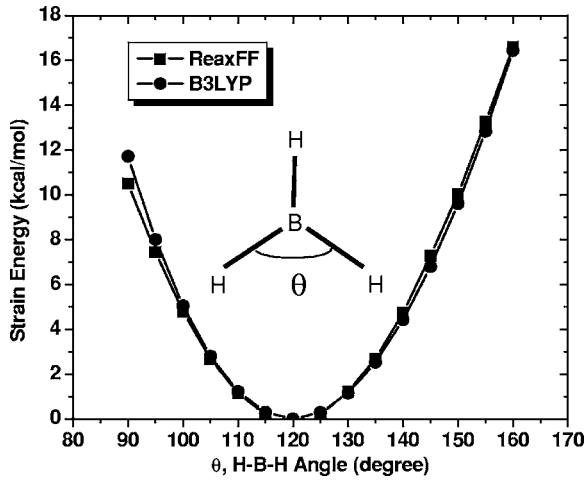

FIG. 2. B3LYP and $ReaxFF_{HBN}$ data for angle distortion of H–B–H in the BH_3 cluster.

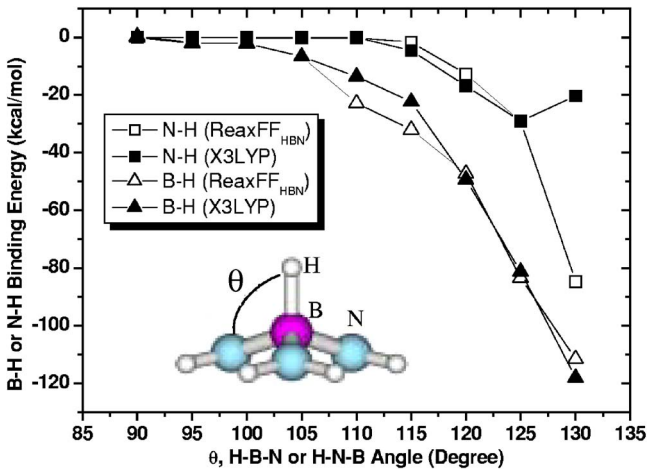

FIG. 3. X3LYP (filled) and $ReaxFF_{HBN}$ (opened) results on B–H (triangle) and N–H (square) bond energies in $H-B(NH_2)_3$ and $H-N(BH_2)_3$ clusters as a function of the out-of-plane angle. The inset displays the H–B–N angle θ in the $H-B(NH_2)_3$ cluster where red, blue, and white atoms mean boron, nitrogen, and hydrogen, respectively.

through DFT calculations. In this work, the EEM method for calculating atomic charges is used because it is one of the fastest methods.[45] The EEM charge deviation method is similar to the QEq scheme;[46] the only difference, apart from the definition of their parameters, is that EEM does not use an iterative scheme for hydrogen charges while QEq uses a more rigorous iterative scheme using Slater orbitals to account for charge overlap. However, the shielding radius γ can be optimized to reproduce the QEq orbital overlap correction.

For a borazine molecule, we find that the $ReaxFF_{HBN}$ atomic charges for the B, N, and H for B–H, and H for N–H of 0.699, −0.874, −0.210, and 0.196 agree with the CHELPG charges of 0.660, −0.768, −0.200, and 0.310, respectively. Likewise, it is determined that in the case of a H_2B-NH_2 the $ReaxFF_{HBN}$ charges for B and N of 0.470 and −0.857 are in reasonably good agreement with the DFT values of 0.488 and −0.824, respectively. On the other hand, it is observed that the $ReaxFF_{HBN}$ partial charges for B of 0.542 and N of −0.757 in the HB═NH is found to be a little different from the CHELPG charges of 0.438 and −0.871, respectively.

D. Out-of-plane effect on B–H and N–H binding energies of planar clusters

B and N atoms in the BNNT may show different chemical properties from those of planar BN structures as the nanotube is curved. In order to investigate the curvature effect, we determine the B–H and N–H bond energies for $H-B(NH_2)_3$ and $H-N(BH_2)_3$ clusters as a function of out-of-plane degree using DFT, as indicated in Fig. 3. In these DFT calculations, we use the extended hybrid functional combined with Lee-Yang-Parr correlation functional (X3LYP),[47] instead of the B3LYP since the X3LYP was reported to describe well hydrogen-bonded and van der Waals complexes more accurately than any other DFT functional.[47]

The geometries of $H-B(NH_2)_3$ and $H-N(BH_2)_3$ clusters are fully optimized while freezing all atoms except a hydrogen atom on the top of B or N. The ground states of both $B(NH_2)_3$ and $N(BH_2)_3$ clusters are in all planar structures. When the $B(NH_2)_3$ and $N(BH_2)_3$ are in planar structures, a hydrogen radical binds weakly with the B atom in $B(NH_2)_3$ and the N atom in $N(BH_2)_3$ where the B–H and N–H binding energies calculated by the X3LYP functional are −0.09 and −0.02 kcal/mol, respectively; however, the B3LYP functional indicates that both of the B–H and N–H bond energies are positive. The B–H and N–H bonds are found to become more stable with increasing H–B–N and H–N–B angles for all of the X3LYP and B3LYP. For instance, when the H–B–N angle in the $H-B(NH_2)_3$ cluster is 130°, the B–H bond energy by the X3LYP is −118.1 kcal/mol, similar to the −115.7 kcal/mol obtained from B3LYP. We find that the lengths of B–H and N–H bonds decreased with an out-of-plane degree of the clusters. When angles of H–B–N and H–N–B are 130°, the B–H bond length of 1.20 Å is found similar to the 1.19 Å in the case of BH_3. Also the N–H bond length of 1.02 Å is predicted to be similar to the 1.01 Å for NH_3. Formation of B–H and N–H bonds makes hybridization at the centered B and N atoms changed from sp^2 to sp^3 and it is possible when angles of H–B–N and H–N–B are above 105° and 115°, respectively. We additionally find that the B–H binding energy is stronger than the N–H binding energy at the same out-of-plane degree.

The reason for the formation of a B–H bond is explained from molecular orbitals for $B(NH_2)_3$ clusters. The lowest unoccupied molecular orbital (LUMO) for a planar $B(NH_2)_3$ cluster with a D_{3h} symmetry is distributed near three nitrogen atoms, while in the $B(NH_2)_3$ cluster with a C_{3v} symmetry the LUMO is distributed around the centered B atom. Based on these results, the charge distribution for the LUMO of $B(NH_2)_3$ is considered to be moved into the centered B atom with the increased out-of-plane degree of the cluster. Therefore, a hydrogen atom is able to make a chemically strong bond with a B atom in $B(NH_2)_3$ if the out-of-plane degree is

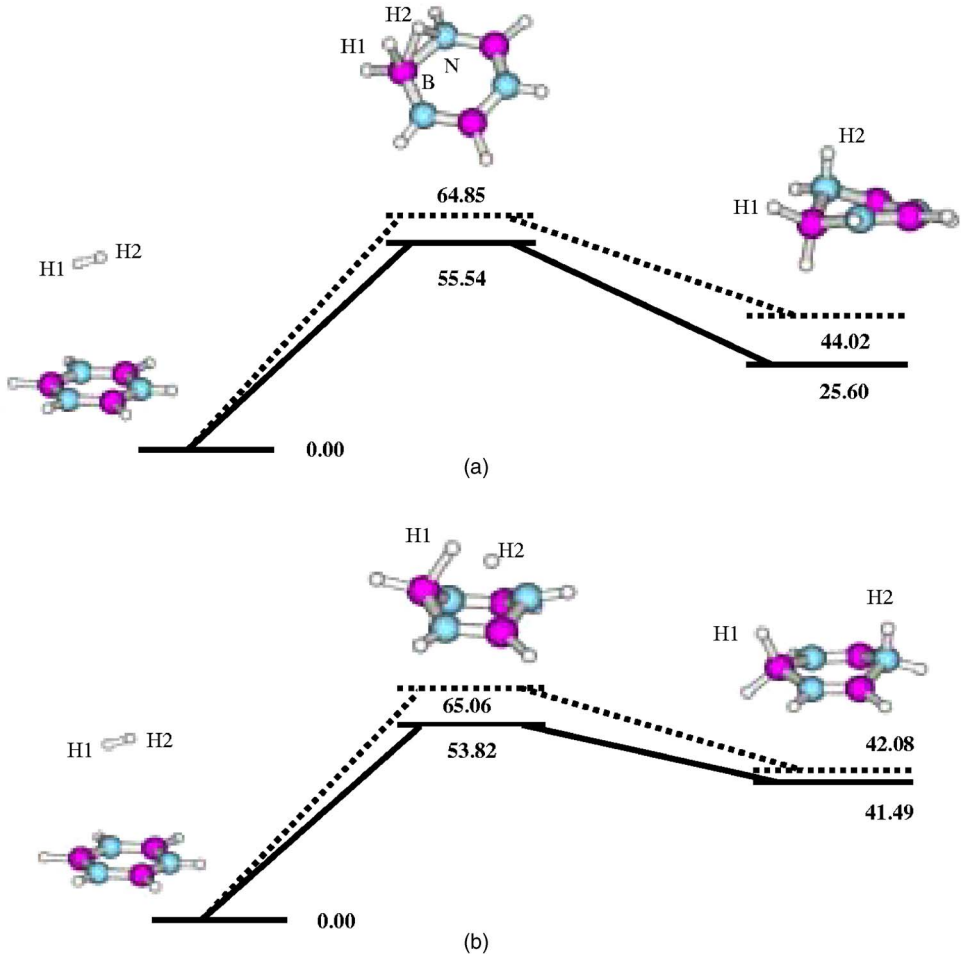

FIG. 4. Pathways for the chemical reaction $B_3N_3H_6$ (borazine)$+H_2 \rightarrow B_3N_3H_8$; (a) when two hydrogen atoms bond chemically with two adjacent B and N atoms of the borazine, and (b) when two hydrogen atoms are bonded with two B and N atoms opposite to each other, where the geometries are obtained from B3LYP DFT calculations. The bold and dot lines indicate the reaction pathways obtained from B3LYP and $ReaxFF_{HBN}$, respectively, where red, blue, and white atoms mean boron, nitrogen, and hydrogen, respectively.

very high. In the case of $N(BH_2)_3$, formation of a N–H bond shows the similar behavior to the case of $B(NH_2)_3$.

$ReaxFF_{HBN}$ is also found to describe correctly the B–H and N–H binding energies in $H-B(NH_2)_3$ and $H-N(BH_2)_3$ with an out-of-plane degree of the clusters. In the case of $H-B(NH_2)_3$, $ReaxFF_{HBN}$ indicates that a B–H bond is formed when the H–B–N angle is larger than 105°, in good agreement with the X3LYP results, as shown in Fig. 3. With the $ReaxFF_{HBN}$, B–H bond energies in the clusters with H–B–N angles of 105° and 130° are −6.6 and −111.6 kcal/mol, respectively, which compares to the X3LYP values of −6.59 kcal/mol with 105° and of −118.1 kcal/mol with 130°. Also, in the case of $H-N(BH_2)_3$, $ReaxFF_{HBN}$ describes correctly N–H binding energies as a function of the out-of-plane degree of the cluster. Therefore, $ReaxFF_{HBN}$ is considered to give the correct interaction between the planar BN systems and hydrogen,but also the correct interaction between the curved BN systems and hydrogen.

E. $B_3N_3H_6$ (borazine)$+H_2 \rightarrow B_3N_3H_8$ reaction mechanisms

The chemical reaction of $B_3N_3H_6$ (borazine)$+H_2 \rightarrow B_3N_3H_8$ is used to model hydrogen adsorption behaviors on the BNNT. We consider two cases as reaction products ($B_3N_3H_8$): a single hydrogen molecule bonds with (a) adjacent B and N atoms in the borazine, and (b) B and N atoms in the opposite direction to each other, as shown in Fig. 4. In the case (a), the B3LYP method predicts that it has the endothermic reaction energy of 25.60 kcal/mol with an activation barrier of 55.54 kcal/mol. In this reaction, any hydrogen atom of a hydrogen molecule bonds to a boron atom in a borazine through the simultaneous dissociation of a hydrogen molecule. On the other hand, it is predicted that the $ReaxFF_{HBN}$ barrier of 64.85 kcal/mol overestimates the B3LYP barrier by 9.31 kcal/mol. Moreover, we also find that the $ReaxFF_{HBN}$ barrier overestimates the B3LYP of 53.82 kcal/mol by 11.24 kcal/mol for the case (b). However, it should be noted that the B3LYP was reported to predict the underestimating tendency for activation barriers.[48–50] In addition, we find that the $ReaxFF_{HBN}$ reaction energy of 42.08 kcal/mol is in close agreement with the B3LYP value of 41.49 kcal/mol.

F. BN crystal properties

The ability of $ReaxFF_{HBN}$ to give correct BN condensed phases stabilities is also tested against *h*-BN and the *c*-BN crystals. For each phase, the DFT energies are obtained from the crystal structures with a broad range of compression and expansion, and then compared to values from the $ReaxFF_{HBN}$, as shown in Fig. 5. In addition the crystal lattice parameters and phase stabilities for each phase are analyzed, as shown in Table IX. The *h*-BN crystal is predicted to be more stable than the *c*-BN one at zero pressure and kelvin,

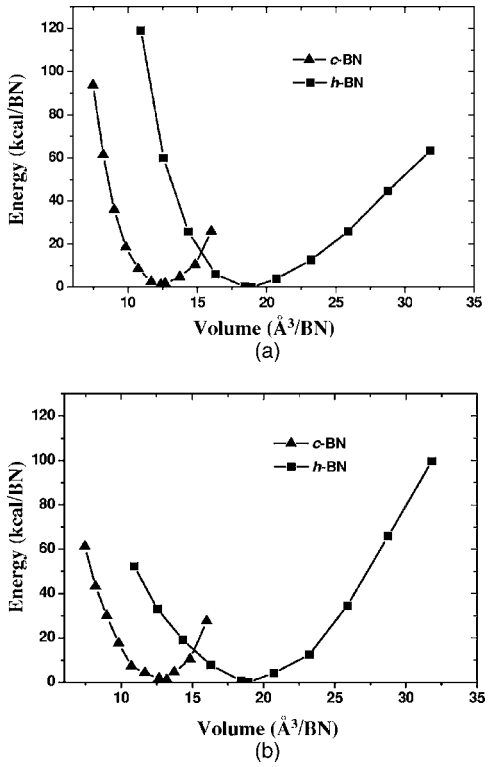

FIG. 5. Equations of states for compression and tension of *h*-BN and *c*-BN crystals, calculated using the (a) PW91 and (b) $ReaxFF_{HBN}$ methods.

which agrees with previous studies.[5,53–55] The DFT cohesive energy of the *c*-BN crystal is 1.27 kcal/BN lower than that of the *h*-BN one, while the $ReaxFF_{HBN}$ describes that the *h*-BN crystal is 0.70 kcal/BN more stable than the *c*-BN one. Both of the DFT (PW91 functional) and $ReaxFF_{HBN}$ indicate that the *h*-BN phase is calculated to be transformed into a *c*-BN crystal in the high compression region where the transition point is about 15 $Å^3$/BN. Also, the $ReaxFF_{HBN}$ is seen to accurately describe DFT lattice parameters of the *h*-BN phase, however, it overestimate the lattice parameter (3.75 Å) of the *c*-BN with the margin of 2.2% compared with the DFT result (3.67 Å).

Finally, we give guidelines of $ReaxFF_{HBN}$ developed in this work because it may have certain limits in its applicability. The present $ReaxFF_{HBN}$ may be considered to be not working far outside our training set. For example, the $ReaxFF_{HBN}$ may not give accurate description for a *w*-BN, a *r*-BN, and various boron hydride crystals which are outside a realm of the present work. Nevertheless, $ReaxFF_{HBN}$ is expected to give the reliable adsorption behaviors of hydrogen on the BNNT wall. It estimates that the reaction for chemical adsorption of hydrogen on the (10,0) SWBNNT exterior wall is endothermic by 25.3 kcal/mol which is almost similar to the value from the DFT (Ref. 56) result of 25.8 kcal/mol.[57] Also, the $ReaxFF_{HBN}$ binding energies of B–H and N–H bonds on the exterior wall of the BNNT are −8.1 and 7.3 kcal/mol, respectively, which are comparable to the DFT values of −13.1 and 4.6 kcal/mol, respectively.[57]

TABLE IX. Lattice parameters for *h*-BN and *c*-BN crystals and phase stabilities for the *c*-BN relative to the *h*-BN, determined through calculations using DFT and $ReaxFF_{HBN}$.

	Lattice parameter (Å)		
Crystal structure	PW91	$ReaxFF_{HBN}$	Expt.
h-BN	*a*:2.52, *c*:6.86	*a*:2.51, *c*:6.83	*a*:2.50,[a] *c*:6.66[b]
c-BN	3.67	3.75	3.62[b]
	Phase stability (kcal/BN)		
c-BN	1.27	0.70	...

[a]Taken from Ref. 51.
[b]Taken from Ref. 52.

IV. CONCLUSIONS

The present work presents the new reactive force field, $ReaxFF_{HBN}$, developed to allow an accurate description of the chemical and physical interactions for large molecular and condensed phase systems of H, B, and N atoms. The very good agreement with DFT calculations is observed for (i) B–H and N–H bond energies of various cluster systems, (ii) the chemical reaction for $B_3N_3H_6+H_2 \rightarrow B_3N_3H_8$, and (iii) crystal properties and physical interaction for *h*-BN and *c*-BN crystals. Consequently, the present $ReaxFF_{HBN}$ is considered to give an accurate description of the chemical and physical processes, thus presenting a great opportunity to be used for multiscale simulations for large systems of B, N, and H atoms. Our test even using only the one-CPU LINUX machine shows that it is trivial to be capable of determining optimized structures and energies for about a few thousand elements of hydrogen, boron, and nitrogen atoms, as well as dynamic simulations at elevated temperature and pressure, thus opening up new possibilities for the role of computational chemistry in materials science.

ACKNOWLEDGMENTS

This research was supported by a grant (Code No. 04K1501-02210) from "Center for Nanostructured Materials Technology" under "21st Century Frontier R&D Programs" of the Korean Ministry of Science and Technology.

APPENDIX: THE $ReaxFF_{HBN}$ PARAMETERS OPTIMIZED FROM DFT DATA FOR VARIOUS MOLECULES AND CONDENSED PHASES OF H, B, AND N ATOMS

The $ReaxFF_{HBN}$ parameters optimized in this work are indicated in Tables I–VII. There, the symbols of the parameters are shown in Refs. 23 and 24.

[1] J. A. Pople, M. Head-Gordon, and K. Raghavachari, J. Chem. Phys. **87**, 5968 (1987).
[2] A. D. Becke, J. Chem. Phys. **98**, 5648 (1993).
[3] N. G. Chopra, R. J. Luyken, K. Cherrey, V. H. Crespi, M. L. Cohen, S. G. Louie, and A. Zettl, Science **269**, 966 (1995).
[4] L. Bourgeois, Y. Bando, W. Q. Han, and T. Sato, Phys. Rev. B **61**, 7686 (2000).
[5] K. Albe, Phys. Rev. B **55**, 6203 (1997).
[6] J. Furthmüller, T. Hafner, and G. Kresse, Phys. Rev. B **50**, 15606 (1994).
[7] F. R. Corrigan and F. P. Bundy, J. Chem. Phys. **63**, 3812 (1975).
[8] X. Blase, A. Rubio, S. G. Louie, and M. L. Cohen, Phys. Rev. B **51**, 6868 (1995).
[9] X. Blase, J.-C. Charlier, A. De Vita, and R. Car, Appl. Phys. Lett. **70**, 197 (1997).

[10] I. Narita and T. Oku, Diamond Relat. Mater. **11**, 945 (2002).
[11] T. Oku, M. Kuno, and I. Narita, J. Phys. Chem. Solids **65**, 549 (2004).
[12] R. Ma, Y. Bando, H. Zhu, T. Sato, C. Xu, and D. Wu, J. Am. Chem. Soc. **124**, 7672 (2002).
[13] C. Tang, Y. Bando, X. Ding, S. Qi, and D. Golberg, J. Am. Chem. Soc. **124**, 14550 (2002).
[14] R. Q. Zhang, T. S. Chu, C. S. Lee, and S. T. Lee, J. Phys. Chem. B **104**, 6761 (2000).
[15] S. Ulrich, J. Scherer, J. Schwan, I. Baren, K. Jung, M. Scheib, and H. Erhardt, Appl. Phys. Lett. **68**, 909 (1996).
[16] D. J. Kester and R. Messier, J. Appl. Phys. **72**, 504 (1992).
[17] T. A. Friedmann, P. B. Mirkarimi, D. L. Medlin *et al.*, J. Appl. Phys. **76**, 3088 (1994).
[18] W. Fukarek, O. Kruse, A. Kolitsch, and W. Moller, Thin Solid Films **308–309**, 38 (1997).
[19] M. Plass, W. Fukarek, A. Kolitsch, and W. Moller, Diamond Relat. Mater. **6**, 594 (1997).
[20] S. J. Harris, G. L. Doll, D. C. Chance, and A. M. Weiner, Appl. Phys. Lett. **67**, 2314 (1995).
[21] S. L. Mayo, B. D. Olafson, and W. A. Goddard III, J. Phys. Chem. **94**, 8897 (1990).
[22] A. K. Rappé, C. J. Casewit, K. S. Colwell, W. A. Goddard III, and W. N. Skiff, J. Am. Chem. Soc. **114**, 10024 (1992).
[23] A. C. T. van Duin, S. Dasgupta, F. Lorant, and W. A. Goddard III, J. Phys. Chem. A **105**, 9396 (2001).
[24] A. C. T. van Duin, A. Strachan, S. Stewman, Q. Zhang, X. Xu, and W. A. Goddard III, J. Phys. Chem. A **107**, 3803 (2003).
[25] A. Strachan, A. C. T. van Duin, D. Chakraborty, S. Dasgupta, and W. A. Goddard III, Phys. Rev. Lett. **91**, 098301 (2003).
[26] Q. Zhang, T. Çağin, A. C. T. van Duin, W. A. Goddard III, Y. Qi, and L. G. Hector, Phys. Rev. B **69**, 045423 (2004).
[27] JAGUAR 4.2, Schrödinger, Inc., Portland, OR, 1991–2000.
[28] R. Krishnan, J. S. Binkley, R. Seeger, and J. A. Pople, J. Chem. Phys. **72**, 650 (1980).
[29] J. P. Perdew and Y. Wang, Phys. Rev. B **45**, 13244 (1992).
[30] N. Troullier and J. L. Martins, Phys. Rev. B **43**, 1993 (1991).
[31] M. C. Payne, M. P. Teter, D. C. Allan, T. A. Arias, and J. D. Joannopoulos, Rev. Mod. Phys. **64**, 1045 (1992).
[32] H. J. Monkhorst and J. D. Pack, Phys. Rev. B **13**, 5188 (1976).
[33] A. C. T. van Duin, J. M. A. Baas, and B. van de Graaf, J. Chem. Soc., Faraday Trans. **90**, 2881 (1994).
[34] See EPAPS Document No. E-JCPSA6-123-711529 for comparisons of DFT and $\text{ReaxFF}_{\text{HBN}}$ results for bond dissociation curves in BH_3, borazine($B_3N_3H_6$), BH_4, H_2B-NH_2, and $HB{=}NH$ clusters and angle distortions in $H_2B-NH-BH_2$, $H_2N-BH-NH_2$, and borazine. This document can be reached via a direct link in the online article's HTML reference section or via the EPAPS homepage (http://www.aip.org/pubservs/epaps.html).
[35] M. C. R. Symons, T. Chen, and C. Glidewell, J. Chem. Soc., Chem. Commun. **326**, (1983).
[36] T. A. Claxton, T. Chen, and M. C. R. Symons, Faraday Discuss. Chem. Soc. **78**, 121 (1984).
[37] R. J. Van Zee, A. P. Williams, and W. Weltner, Jr., J. Chem. Phys. **107**, 4756 (1997).
[38] A. I. Boldyrev and J. Simons, J. Chem. Phys. **99**, 4629 (1993).
[39] H. B. Schlegel, A. G. Baboul, and S. J. Harris, J. Phys. Chem. **100**, 9774 (1996).
[40] L. Andrews and X. Wang, J. Am. Chem. Soc. **124**, 7280 (2002).
[41] A. Rubio, J. L. Corkill, and M. L. Cohen, Phys. Rev. B **49**, 5081 (1994).
[42] W. J. Mortier, S. K. Ghosh, and S. J. Shankar, J. Am. Chem. Soc. **108**, 4315 (1986).
[43] S.-H. Jhi and Y.-K. Kwon, Phys. Rev. B **69**, 245407 (2004).
[44] C. M. Breneman and K. B. Wiberg, J. Comput. Chem. **11**, 361 (1990).
[45] A. R. Leach, *Molecular Modelling: Principles and Applications* (Pearson Education, England, 2001).
[46] A. K. Rappé and W. A. Goddard III, J. Phys. Chem. **95**, 3358 (1991).
[47] X. Xu and W. A. Goddard III, Proc. Natl. Acad. Sci. U.S.A. **101**, 2673 (2004).
[48] J. K. Kang and C. B. Musgrave, J. Chem. Phys. **115**, 11040 (2001).
[49] B. G. Johnson, C. A. Gonzales, P. M. W. Gill, and J. A. Pople, Chem. Phys. Lett. **221**, 100 (1994).
[50] B. S. Jursic, Chem. Phys. Lett. **256**, 603 (1996).
[51] V. L. Solozhenko, G. Will, and F. Elf, Solid State Commun. **96**, 1 (1995).
[52] E. Knittle, R. M. Wentzcovitch, R. Jeanloz, and M. L. Cohen, Nature (London) **337**, 349 (1989).
[53] T. E. Mosuang and J. E. Lowther, J. Phys. Chem. Solids **63**, 363 (2002).
[54] E. Kim and C. Chen, Phys. Lett. A **319**, 384 (2003).
[55] A. Janotti, S.-H. Wei, and D. J. Singh, Phys. Rev. B **64**, 174107 (2001).
[56] The DMOl3 software was used and the calculation was performed at the BLYP level with double numerical polarized (DNP) basis set.
[57] S. S. Han, J. K. Kang, H. M. Lee, A. C. T. van Duin, and W. A. Goddard III, J. Chem. Phys. **123**, 114704 (2005), following paper.